

Investigation of the Combination of Chicken Feathers and Polyhydroxyalkanoates for Sustainable and Biodegradable Composite Materials

Nayan Vaghasiya, Jens Schuster, Chandrasekhar Kode

Department of Applied Logistics and Polymer Sciences, University of Applied Sciences Kaiserslautern, Pirmasens, Germany
Email: nava1002@stud.hs-kl.de

How to cite this paper: Vaghasiya, N., Schuster, J. and Kode, C. (2026) Investigation of the Combination of Chicken Feathers and Polyhydroxyalkanoates for Sustainable and Biodegradable Composite Materials. *Open Journal of Composite Materials*, 16, 1-22.

<https://doi.org/10.4236/ojcm.2026.161001>

Received: November 5, 2025

Accepted: December 27, 2025

Published: December 30, 2025

Copyright © 2026 by author(s) and Scientific Research Publishing Inc.

This work is licensed under the Creative Commons Attribution-NonCommercial International License (CC BY-NC 4.0).

<http://creativecommons.org/licenses/by-nc/4.0/>



Open Access

Abstract

This study investigated the development of a sustainable and biodegradable composite material reinforced with chicken feathers and based on polyhydroxyalkanoates (PHAs), a family of thermoplastic polyesters that naturally decompose. PHAlife™ PB3430G was used as the matrix, while chicken feathers were processed into powder (CFP) and fiber (CFF) forms and incorporated at 10% and 20% loadings. To improve compatibility between the hydrophilic keratin and hydrophobic PHA, the feathers were modified through alkali and silane treatments. Composites were fabricated using a twin-screw extruder and hot-press compression molding and subsequently characterized for their mechanical, physical, and morphological properties. The results showed that CFF at 20% loading provided the most effective reinforcement, significantly enhancing tensile and compressive strength compared to CFP, while density measurements confirmed the lightweight nature of the composites. At lower filler concentrations, microscopy revealed improved interfacial adhesion and better filler dispersion. The silane coupling agent chemically bonded the chicken feather fillers to the PHA matrix, enhancing interfacial adhesion. Overall, the findings suggest that chicken feather waste can be effectively utilized as an affordable reinforcement for PHA-based composites, offering a promising route to produce strong, lightweight, and environmentally friendly materials for biodegradable consumer products, single-use disposables, and horticultural applications.

Keywords

Chicken Feathers, Polyhydroxyalkanoates (PHA), Biodegradable Composites, Keratin Fibers, Bio-Based Materials, Surface Modification, Waste Valorization, Carbon Footprint Reduction, Natural Fiber

1. Introduction

Growing concerns over plastic waste have increased interest in biodegradable alternatives such as polyhydroxyalkanoates (PHAs). Although PHAs are biodegradable and microbially produced, their wider use is limited by the high cost of production [1] and by mechanical drawbacks, especially the stiffness and brittleness of PHB-rich grades [2]. At the same time, the poultry industry generates millions of tons of chicken feathers annually, creating financial and environmental challenges when these wastes are disposed of through landfilling or incineration [3]. Chicken feathers, rich in keratin and naturally resistant to degradation, have been explored as renewable fillers that provide lightweight and biodegradable reinforcement for fully biodegradable biocomposites with high feather content [4]. The present study aims to investigate the incorporation of chicken feathers into PHA matrices as a renewable reinforcement strategy to reduce dependence on petroleum-based polymers while maintaining or improving composite performance.

The incorporation of natural fibers and bio-based fillers into polymers has been extensively studied to enhance mechanical, thermal, and environmental performance while supporting sustainability objectives. Chicken feathers consist of approximately 85% - 90% β -keratin—a fibrous structural protein rich in cysteine residues that form disulfide crosslinks, providing significant strength and chemical stability [5]. Their hollow, honeycomb-like morphology contributes to an exceptionally low apparent density, making chicken feathers attractive lightweight fillers for polymer composites [6]. Barone and Schmidt first demonstrated the reinforcing potential of keratin fibers in polyethylene, establishing the foundation for their application in composite materials [7]. However, Azam Ali *et al.* highlighted that the hydrophilic natural fibers hinder effective bonding with hydrophobic polymer matrices [8], while Khan *et al.* emphasized the importance of fiber-matrix adhesion, chemical treatment, and optimized processing parameters [9]. Chemical surface treatments are often used to improve the interfacial compatibility between natural fillers and polymer matrices [10]. Alkali treatment is expected to remove surface impurities and expose reactive $-OH$ and $-NH_2$ groups on keratin, while silane coupling agents can form a molecular bridge, with the hydrolyzable group ($-Si-OR$) reacting with keratin and the organofunctional group interacting with PHA. This mechanism can improve interfacial adhesion, stress transfer, and overall composite performance. Ali *et al.* reported that surface-treated chicken feathers significantly enhanced the tensile strength of unsaturated polyester composites, highlighting the benefits of treatment and filler incorporation [11]. Jiménez-Cervantes *et al.* found that the chicken feather quill exhibited excellent compatibility with the polypropylene matrix, these findings are directly applicable to PHA feather matrix [12]. S. V. Bharathi observed that feather barbs

possess a higher slenderness ratio/aspect ratio than the rachis, leading [13]. Similarly, Reddy and Yang highlighted the unique hollow honeycomb structure, low density, high flexibility, and distinctive protein crystal morphology of chicken feather barbs [5]. Xie *et al.* reviewed silane coupling agents for natural fiber and polymer composites, confirming that silane treatments improve interfacial adhesion with polymers like HDPE by forming chemical bridges [14]. Oladele *et al.* investigated NaOH-treated chicken feather fibers in HDPE composites and analyzed their crystallinity and morphology, which are critical factors influencing composite performance [15]. Pasayev and Cadir reported that cleaning and defatting remove surface contaminants and lipids, producing odor-free fibers with enhanced compatibility [16]. Khan *et al.* (2022) further reviewed how feather properties, including particle size, volume fraction, and surface modification, govern the mechanical, physical, and thermal behavior of composites [9]. Cheng *et al.* demonstrated that sequential twin-screw extrusion and molding achieve homogeneous dispersion of chicken-feather fibers in PLA composites, leading to PHA-feather composite [17]. Touatou and Belhaneche-Bensemra investigated PVC composites containing untreated chicken-feather fibers and observed only minor improvements in mechanical properties, indicating that chemical treatments are required to enhance fiber-matrix adhesion and overall composite strength [18]. Aranberri *et al.* [4] examined biodegradable composites with high feather loadings and reported reduced density but diminished strength due to agglomeration and poor dispersion.

Building on these insights, this study aims to demonstrate how feather morphology, filler concentration, and chemical surface treatment influence the mechanical and physical properties of PHA-based biodegradable composites. Chicken feathers were processed as fibers (CFF) and powders (CFP) at 10% and 20% weight fractions, with alkali and silane coupling treatments applied to improve interfacial adhesion between the hydrophilic keratin and hydrophobic PHA matrix. The effects of these variables were systematically evaluated through tensile and compressive testing, hardness and density measurements, and microscopic analysis, providing insights into the potential of chicken feather waste as a sustainable reinforcement for biodegradable polymer composites.

2. Materials and Methods

2.1. Chicken Feathers

In this study, chicken feathers were used as a natural reinforcement material. They were sourced from poultry processing facilities in Pirmasens, Germany. As shown in **Figure 1(a)**, chicken feathers exhibit a hierarchical structure that contributes to their unique mechanical properties. Barbs extend from the central rachis, with barbules branching out and terminating in hook-like tips that interlock adjacent structures [5]. **Figure 1(b)** illustrates the hollow, honeycomb-like internal structure of individual barbs, which reduces density while maintaining strength [5].

The barbs possess high aspect ratios (346.7 ± 4.0 for males and 336.3 ± 2.2 for

females) and fineness values of 84.2 ± 2.4 (male) and 81.7 ± 2.8 (female), indicating their suitability for processing as natural fibers [13]. These characteristics make feather barbs effective reinforcements for PHA composites. Chicken feathers contain approximately 90% keratin protein, making them a valuable source for keratin-based fiber compounds. The remaining chemical composition includes a moisture content of approximately 12.3%, along with smaller fractions of crude fiber (2.2%), ash (1.5%), crude lipid (0.8%), and nitrogen-free extract (1.0%) [19].

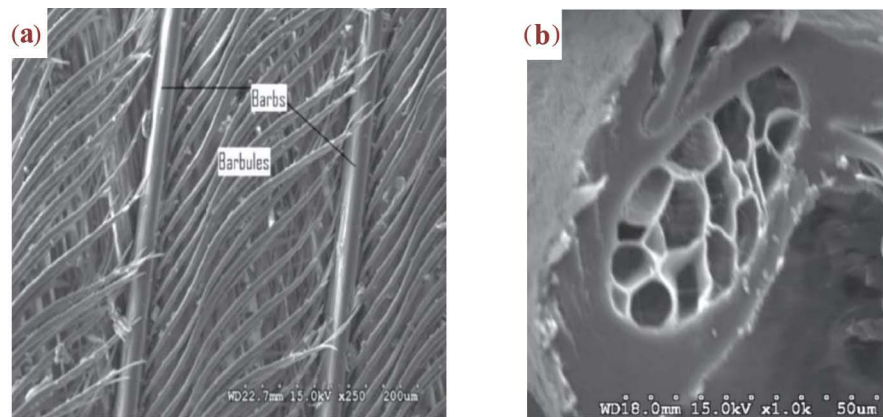


Figure 1. SEM images of chicken feather microstructure: (a) Tertiary structure of barbs and barbules [5], (b) Cross-sectional view of a barb showing hollow honeycomb features [5].

2.1.1. Properties of Chicken Feather Barbs and Powders

Chicken feathers were utilized in fiber form (CFF), providing a distinct set of physical and mechanical properties suitable for bio-composite reinforcement.

- Feather Fibers (barbs): Retain the native keratin structure, offering low density (approximately 0.8 g/cm^3) and high mechanical performance. They exhibit high tensile strength ($187.2 \pm 59.8 \text{ MPa}$), a high Young's modulus ($4.6 \pm 1.6 \text{ GPa}$), and low elongation at break ($7.7 \pm 0.9\%$), making them inherently brittle [5]. These characteristics make CFF ideal as rigid reinforcement in biocomposite matrices.
- Feather Powder: Produced by milling feathers, this process disrupts the native fibrous structure, resulting in higher surface area and improved dispersion within the polymer matrix.

These properties support the strategic selection of CFF for mechanical reinforcement and CFP as a lightweight filler in a PHA composite matrix.

2.1.2. Extraction of Fibers

Chicken feathers were initially sorted to remove damaged or soiled samples, as well as the thick or brittle portions of the rachis, ensuring uniform quality. The brittle sections were discarded because they can act as stress concentrators and potentially induce fractures within the composite. The remaining flexible fibrous regions, including the intact rachis, barbs, and barbules, were retained to provide favorable mechanical and structural properties for reinforcement in composite materials. **Figure 2** shows the cleaned chicken feathers obtained after removing

the brittle and thicker rachis portions.



Figure 2. Cleaned chicken feathers.

2.1.3. Alkali Treatment

To further improve the surface characteristics and interfacial compatibility of the fibers, an alkali treatment was performed using a 3% - 4% potassium hydroxide (KOH) solution. As shown in **Figure 3(a)**, the cleaned chicken feathers were immersed in the KOH solution to initiate surface modification. The immersion process allowed the alkali solution to penetrate and react with the keratin structure. In **Figure 3(b)**, the feathers were gently stirred in the solution for 4 hours at room temperature to ensure uniform treatment and effective removal of surface impurities.

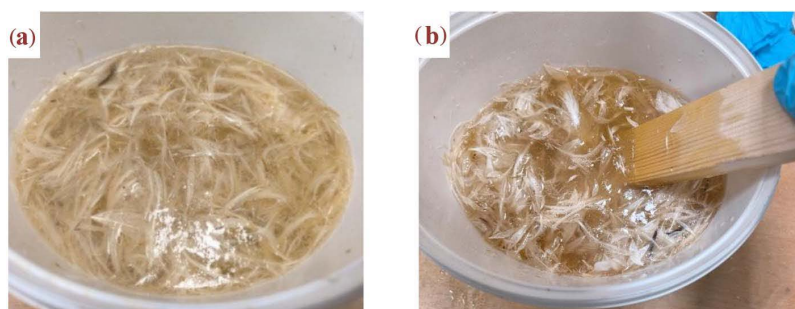


Figure 3. Alkali treatment process of chicken feathers: (a) Immersion of feathers in KOH solution, (b) Stirring of feathers during treatment.

This treatment removed residual lipids and pigments while increasing surface roughness, thereby facilitating mechanical interlocking and enhancing adhesion between the hydrophilic keratin fibers and the hydrophobic PHA matrix. Following treatment, the fibers were rinsed thoroughly with distilled water and then dried in an oven at 45°C for 40 hours to remove moisture, prevent microbial growth, and stabilize the keratin structure.

2.1.4. Grinding

After drying, the alkali-treated feather fibers were subjected to mechanical grinding to convert them into fine powders. A high-speed grinder operating at 35,000 rpm was used for this process. The grinding time was adjusted depending on the desired form:

- For long fiber production: Grinding for 5 minutes preserved fiber morphology,

producing fibers 5 - 20 mm long and 28 - 50 μm in diameter with a high aspect ratio ($\sim 500 - 1000$) suitable for reinforcement.

- For powder production: Grinding for 25 minutes produced fine particles with a size of approximately 150 - 600 μm , refined with a strainer for uniform size, suitable as a particulate filler.

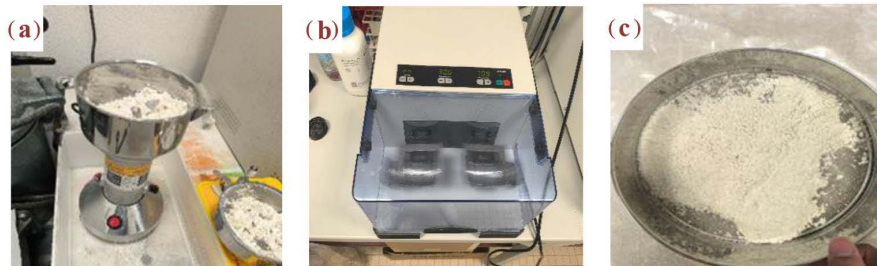


Figure 4. Grinding: (a) Grinder, (b) Ball mill machine, (c) Strainer for fine powder.

As shown in **Figures 4(a)-(c)**, the grinding setup included a high-speed grinder and a ball mill for size reduction, followed by sieving to achieve a uniform particle size distribution. The resulting powder, typically within the 150 - 600 μm range, was subsequently used as a filler in bio-composite formulations.

2.1.5. Surface Treatment of Feathers and Powder

Feather powders and long feathers were modified with 3-aminopropyl triethoxysilane (APTES) to enhance their compatibility with the PHA matrix. The treatment process involved:



Figure 5. Silane treatment of chicken feather powder: (a) (3-aminopropyl) triethoxysilane (APTES), (b) APTES-treated feather powder.

- Soaking the ground feather powders in a 2% APTES solution prepared in ethanol as shown in **Figure 5(a)-(b)**.
- Maintaining the suspension at room temperature for 24 hours allows for adequate surface functionalization.
- Filtering the excess silane and drying the modified powder at 45 °C for 40 hours ensures the complete curing of the silane coating.

The chemical mechanism involves the amino-functional groups of APTES forming covalent bonds with keratin on the feather surface, thereby enhancing

adhesion to the hydrophobic PHA matrix.

2.2. PHA (Polyhydroxyalkanoates)

For this investigation, a polyhydroxyalkanoate (PHA) biopolymer was selected as the matrix material. PHAs comprise a large family of linear polyesters that are both bio-based and biodegradable, naturally produced by various micro-organisms through the fermentation of renewable feedstocks. The general chemical structure of these aliphatic polyesters consists of repeating units of $(-O-CH(R)-CH_2-C(=O)-)$, where the side-chain R group varies, resulting in polymers with characteristics ranging from elastomers to rigid plastics [2].

PHAlife-PB3430G Bio-Based Thermoplastic Polyester

PHAlife™ PB3430G is a commercially available, fully bio-based PHA copolymer designed for industrial applications requiring a balance between flexibility and processability [20]. This grade is a copolymer of 3-hydroxybutyrate (3HB) and 4-hydroxybutyrate (4HB), containing 34% 4HB, which reduces brittleness while maintaining thermal and tensile performance.

Molecular Structure: $(C_8H_{16}O_6)_n$

CAS No.: 125495-90-1

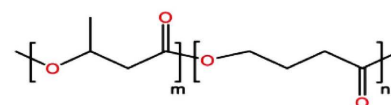


Figure 6. Molecular structure of polyhydroxyalkanoate (PHA) [20].

Table 1. Properties of PHAlife™-PB3430G; Source: Helian Polymers Technical Datasheet [20].

Performance	Index	Unit	Testing Standards
Melting index (175 °C, 2.16 kg)	≤10	g/10 min	ISO 1133
Moisture and volatiles	≤0.5	%	ISO 1269
Melting point	170	°C	DSC
Glass transition temperature	-9 - -7	°C	DSC
Crystallinity	12	%	ISO 11357
Density	1.23	g/cm ³	ISO 1183
Tensile strength	10-15	MPa	ISO 527
Nominal tensile strain at break	≥10	%	ISO 527
Izod impact strength (23 °C)	>5	kJ/m ²	ISO 179
Heat deflection temperature	60 - 70	°C	ISO 75

As shown in **Figure 6**, the molecular structure of polyhydroxyalkanoate (PHA) is illustrated [20]. Chicken feathers can be incorporated into PHA without thermal degradation, making them suitable bio-fillers to enhance composite material properties. The specific properties of PHAlife™ PB3430G are summarized in **Table 1**, including thermal, mechanical, and processability data [20].

2.3. Design of Experiments

To evaluate the effects of chicken feather morphology and concentration on PHA-

based bio-composites, five different formulations were prepared using PHAlife™ PB3430G as the polymer matrix. Chicken feathers were processed into two distinct forms: chicken feather powder (CFP) and chicken feather fibers (CFF). These fillers were incorporated at 10% and 20% loading levels to assess their influence on the mechanical, physical, and thermal properties of the composites. The experimental design is summarized in **Table 2**, which outlines the composition of each formulation.

Table 2. Design of experiments.

Samples	PHA (%)	CFP (%)	CFF (%)
S1	100	-	-
S2	90	10	-
S3	80	20	-
S4	90	-	10
S5	80	-	20

The base material (Sample S1) contained 100% PHA and served as the reference. Samples S2 and S3 incorporated 10% and 20% CFP, respectively, while Samples S4 and S5 contained 10% and 20% CFF. This systematic approach enabled a comparative analysis of how both filler form (powder versus fiber) and concentration affect filler dispersion, matrix-filler interaction, and overall composite properties.

2.4. Compounding

Materials were prepared according to the formulations defined in the design of experiments. PHAlife™ PB3430G pellets were pre-dried to remove residual moisture and then fed into a kneader (IKA-Werke GmbH) set at 178°C and 40 rpm, as shown in **Figure 7(a)**. The PHA granules were allowed to melt for 2 - 2.5 minutes before gradually adding the chicken feather filler (either powder or fiber) according to each formulation. The addition of the filler and initial mixing is illustrated in **Figure 7(b)**, while the final homogeneous compounded materials are shown in **Figure 7(c)**. Mixing was continued for a total of 5-6 minutes to ensure uniform dispersion.

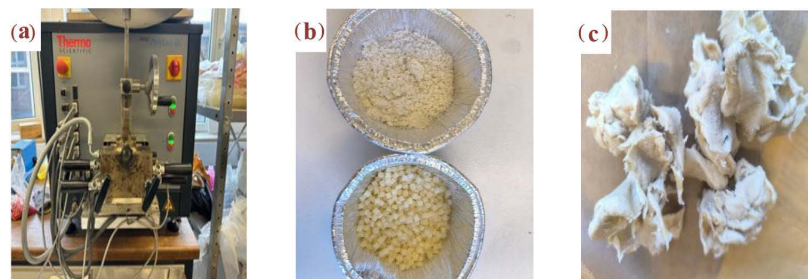


Figure 7. Compounding process of PHA and chicken feather powder: (a) Kneader, (b) PHA granules and CFP/CFF, (c) Compounded materials.

The compounded materials were subsequently passed through a granulator to

produce fine, homogeneous granules, facilitating smoother and more efficient processing during compression molding.

2.5. Compression Molding

Composite granules were formed into test specimens by compression molding using a hot press (Collin P200E), as shown in **Figure 8(a)**, following standard thermoplastic processing procedures (DIN EN ISO 527). The platens and mold were preheated to 175°C - 178°C, consistent with the melt-processing window of the selected PHA grade.

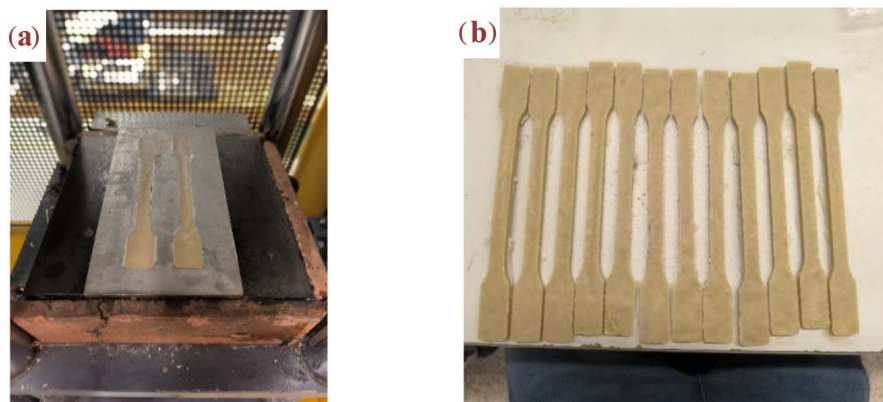


Figure 8. Fabrication of PHA-feather composite specimens: (a) Compression mold, (b) PHA-feather composite specimens.

The composite granules were evenly distributed within the mold cavity, and molding was conducted at a nominal pressure of 15 bar for 5 minutes to ensure complete melting, flow, and wetting of the chicken feather reinforcements. Following the heating and pressing stage, pressure was maintained while the assembly was cooled to ambient temperature over 8 - 10 minutes. Controlled cooling minimized residual stresses and reduced the risk of warpage or microcracking due to thermal contraction. The specimens were then demolded (**Figure 8(b)**).

2.6. Test Equipment and Test Parameters

2.6.1. Tensile Test (Universal Testing Machine)

Tensile tests were performed using a Universal Testing Machine (Zwick Roell) to evaluate the mechanical behavior of the composite materials in accordance with DIN EN ISO 527. Type 1A dog bone specimens (115 × 10 × 5 mm) were used, as shown in **Figure 9(a)**.

The testing parameters were as follows:

- Test Speed: 5 mm/min.
- Grip Type: Mechanical clamps.
- Pre-load: 10 N.
- Young's modulus was determined within a strain range of 0.05% - 0.25%.
- Five specimens were tested per composite formulation, with average values re-

ported.

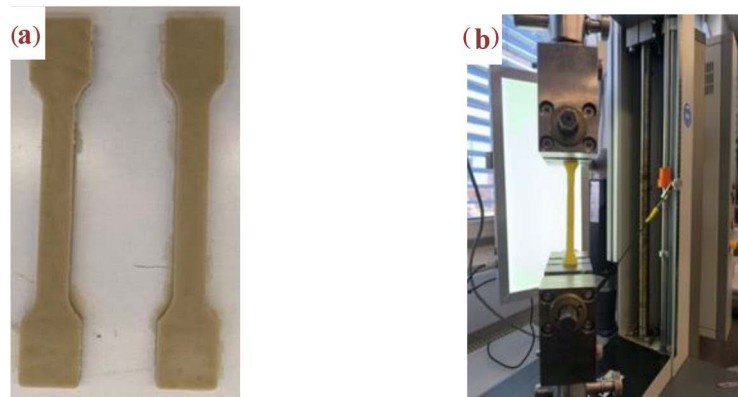


Figure 9. Tensile testing setup: (a) Test specimens, (b) Tensile test equipment.

During testing, force and displacement were continuously recorded to generate stress-strain curves. From these curves, tensile strength, elongation at break, and Young's modulus were determined. The experimental setup is shown in **Figure 9(b)**.

2.6.2. Compression Test

Compression tests were conducted to evaluate the mechanical behavior of the composites under compressive loads. This method provides critical information on material strength, stiffness, and deformation response, which are essential for assessing structural performance and suitability for engineering applications. In this study, tests were performed in accordance with the DIN EN ISO 604 standard, using specimens with dimensions of $5 \times 5 \times 8$ mm to ensure consistency. Testing was carried out at a crosshead speed of 50 mm/min. During the experiments, force and displacement were continuously recorded to generate detailed stress-strain curves.

2.6.3. Impact Resistance Test (Charpy Test)

Impact resistance was evaluated using the Charpy impact test in accordance with DIN EN ISO 179. Test specimens were prepared with dimensions of $80 \times 10 \times 5$ mm and a 2 mm V-notch to create a defined fracture zone. The notching process was performed using a precision notch machine, as shown in **Figure 10(a)**.



Figure 10. Impact testing: (a) Notch preparation machine, (b) Pendulum impact testing machine, (c) Fractured specimens after testing.

The specimens were subsequently tested on a pendulum impact testing machine (Figure 10(b)), and the energy absorbed during fracture was recorded for each sample. After testing, the fractured specimens were collected for further examination of the fracture surfaces (Figure 10(c)).

2.6.4. Hardness Test (Shore A & D Durometer)

The hardness of the composite specimens was measured using both Shore A and Shore D durometers in accordance with DIN EN ISO 868. Shore A was used to evaluate softer composites, whereas Shore D was applied to assess stiffer formulations (Figure 11(a)-(b)).

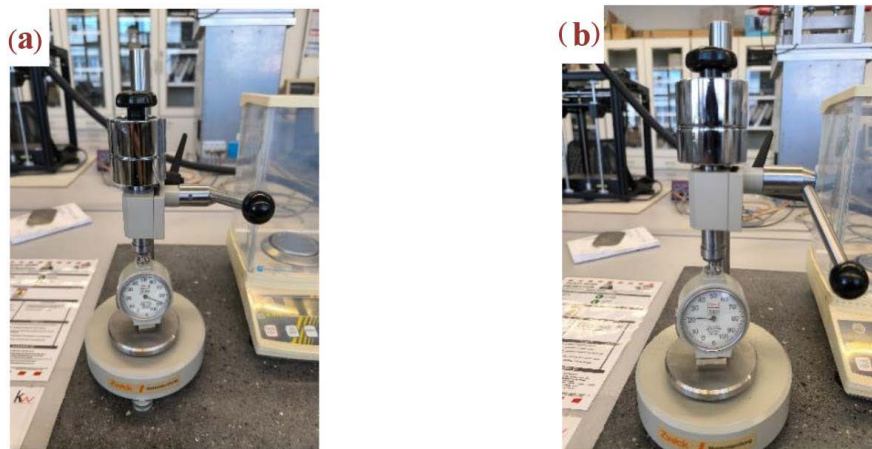


Figure 11. Hardness testing of composite specimens: (a) Shore A hardness test, (b) Shore D hardness test.

For specimens with thicknesses ≤ 6 mm, the indenter was positioned perpendicular to the surface, and a load of 1 kg was applied. Readings were recorded after the standard dwell time, and averages from multiple points were reported to minimize variability. Shore A values reflected the softer response of composites with lower filler content, while Shore D values captured the higher stiffness of rigid samples.

2.6.5. Density Measurement Test (Archimedes' Principle)

Density was determined using Archimedes' Principle in accordance with DIN EN ISO 1183. As illustrated in Figure 12, each specimen was weighed in air and then submerged in distilled water, and the density was calculated using Equation (1).

$$\rho = 1000 \times \frac{W_{air}}{W_{air} - W_{water}} \quad (1)$$

All specimens were free from visible defects or trapped air. The average of multiple measurements was reported. This method provided insights into the composite's structural uniformity and filler dispersion. A noticeable reduction in density was observed in CFF-containing samples, attributed to the low density, porous structure of feathers.



Figure 12. Density Archimedes' principle.

2.6.6. Microscopy

Microscopic analysis was performed to evaluate the morphology of the composites, with particular focus on filler dispersion and void formation. Optical microscopy allowed identification of voids, crack initiation sites, the fiber-matrix interface, and potential particle agglomeration.

3. Results

The incorporation of chicken feather powder (CFP) and chicken feather fiber (CFF) into PHA-based biodegradable composites significantly influenced their mechanical, physical, thermal, and morphological properties. This section presents a detailed analysis of these effects, using both experimental data and visual documentation through figures.

3.1. Tensile Strength

Tensile testing revealed notable differences among the five composite formulations. The neat PHA reference sample (S1) established a baseline tensile strength of 14.5 MPa. As shown in **Figure 13**, the incorporation of 10% CFP (S2) slightly increased the tensile strength to 15.0 MPa, while 20% CFP (S3) resulted in 15.1 MPa. These improvements, ranging from 3.6% to 4.3%, indicate that CFP reinforcement moderately enhances tensile performance. However, S3 exhibited the highest standard deviation (± 2.8 MPa), suggesting variability in mechanical properties, likely due to poor dispersion or weak matrix-particle bonding.

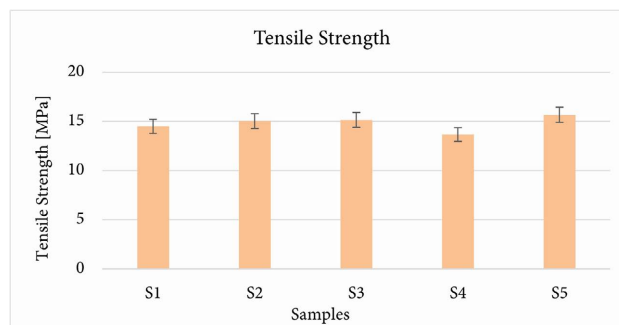


Figure 13. Tensile strength.

In contrast, CFF-reinforced samples exhibited a different trend. Sample S4 (10% CFF) showed the lowest tensile strength (13.7 MPa) but the smallest variation (± 0.9 MPa), indicating a more homogeneous mechanical response. The highest tensile strength was observed in S5 (20% CFF), reaching 15.7 MPa, an 8% increase over neat PHA. This improvement highlights that higher fiber content enhances stress transfer and fiber-matrix interlocking, resulting in more effective reinforcement.

3.2. Young's Modulus

Young's modulus, a measure of material stiffness, further illustrates the effects of feather content and morphology. As shown in **Figure 14**, the neat PHA sample (S1) exhibited a modulus of 428.3 MPa. Sample S2 (10% CFP) showed a substantial increase to 604.7 MPa, approximately 41% higher, indicating that even small amounts of CFP can significantly stiffen the matrix. However, increasing CFP to 20% (S3) reduced the modulus to 493.3 MPa. This reduction is attributed to the agglomeration of the powder, which acts as stress concentration points that disrupt efficient load transfer within the PHA matrix. For CFF composites, Sample S4 (10% CFF) exhibited the lowest modulus of 222.7 MPa, nearly 48% lower than neat PHA. Sample S5 (20% CFF) increased modestly to 342.3 MPa but remained below the reference.

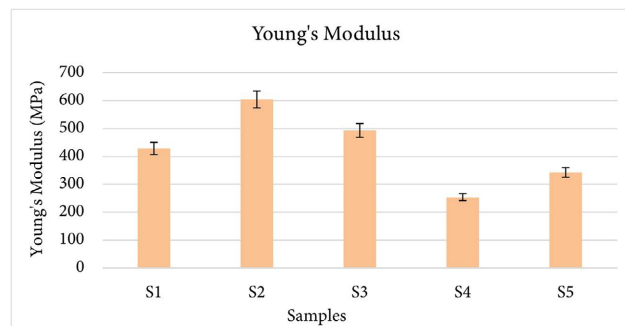


Figure 14. Young's modulus.

The high standard deviation in S5 (± 200.8 MPa) reflects the challenges of achieving uniform fiber dispersion, which strongly influences stiffness. This underscores a key principle in composite design: without optimized dispersion, a potentially reinforcing agent like CFF can paradoxically reduce stiffness by disrupting the polymer matrix more than it reinforces it.

3.3. Impact Strength

Impact strength was evaluated to assess the ability of each formulation to withstand sudden forces. As shown in **Figure 15**, the neat PHA sample (S1) exhibited the highest impact resistance at 47 kJ/m². Incorporation of 10% and 20% CFP (S2 and S3) resulted in significant reductions to 29.9 kJ/m² and 20.4 kJ/m², respectively, indicating increased brittleness and decreased energy absorption with

higher CFP content.

CFF-reinforced composites demonstrated more favorable behavior. Sample S4 (10% CFF) exhibited an impact strength of 38.9 kJ/m², only 17% below the reference, suggesting that fiber reinforcement improves energy dissipation. Sample S5 (20% CFF) showed a comparable impact strength to S3 (20.1 kJ/m²) but with greater consistency. These results indicate that moderate fiber reinforcement maintains toughness more effectively than powder fillers.

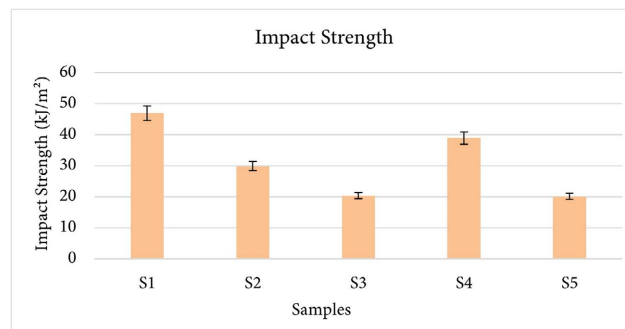


Figure 15. Impact strength.

3.4. Hardness (Shore A & D)

3.4.1. Hardness (Shore A)

Shore A hardness measurements quantified the surface resistance of the composites to indentation. As shown in **Figure 16**, the control sample (S1) recorded an average Shore A hardness of 87.7. Incorporation of 10% CFP (S2) slightly increased the hardness to 88.5, whereas the 20% CFP sample (S3) decreased to 83.7.

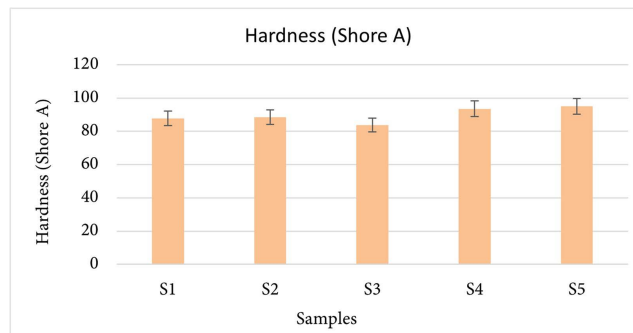


Figure 16. Hardness Shore A.

In contrast, CFF-reinforced composites exhibited notable improvements: S4 (10% CFF) and S5 (20% CFF) achieved hardness values of 93.5 and 95, representing 6.5% and 8.3% increases, respectively. These results indicate that CFF more effectively enhances surface hardness, while CFP performance is limited by concentration-dependent agglomeration.

3.4.2. Hardness (Shore D)

Shore D hardness values of the composites ranged from 25 to 28, with minor var-

iations between formulations (Figure 17). The neat PHA sample (S1) exhibited the highest hardness, averaging 27.5. The 10% CFP composite (S2) showed a slight reduction to approximately 26, while the 20% CFP sample (S3) maintained values near 27. Fiber-reinforced composites (S4 and S5) exhibited intermediate hardness values of 25 - 26, indicating that fiber addition did not substantially enhance surface hardness compared to powder reinforcement. Overall, the minor reduction in Shore D hardness across reinforced samples suggests that the filler-matrix interface represents the primary limitation under sharp indentation.

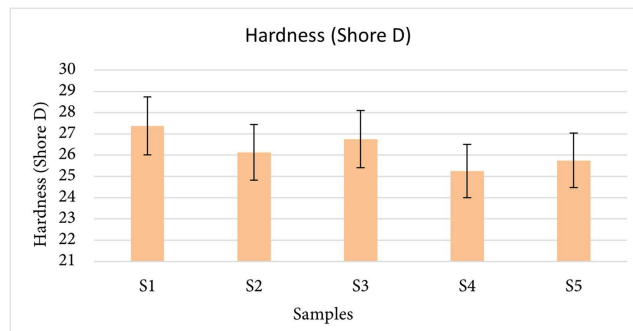


Figure 17. Hardness Shore D.

3.5. Density

Density measurements provide insights into composite compaction and porosity. As shown in Figure 18, the neat PHA sample (S1) exhibited the highest density at 1.227 g/cm^3 . CFP-reinforced composites (S2 and S3) showed slightly lower densities of 1.208 g/cm^3 and 1.207 g/cm^3 , respectively. In contrast, CFF composites exhibited more pronounced reductions in density: 1.191 g/cm^3 for S4 and 1.143 g/cm^3 for S5, representing a 7% decrease relative to S1. These results suggest that CFF introduces greater internal voids or reduces filler packing efficiency, making it a promising option for lightweight applications.

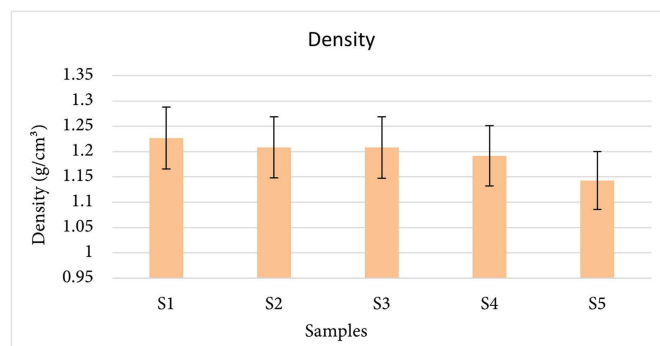


Figure 18. Density.

3.6. Compression Strength

Compression strength results, shown in Figure 19, reveal distinct effects of filler type and concentration. The neat PHA sample (S1) exhibited a compressive

strength of 15.5 MPa. Incorporation of 10% CFP (S2) led to a significant increase to 20.6 MPa, representing a 33% improvement, whereas the 20% CFP sample (S3) decreased to 16.9 MPa. For CFF-reinforced composites, 10% CFF (S4) resulted in a slight reduction to 14.5 MPa, but increasing the fiber content to 20% (S5) improved compressive strength to 20.6 MPa. These findings indicate that well-dispersed CFF at higher loadings effectively enhances compressive strength, attributed to the reinforcing effect of longer fibers with higher aspect ratios.

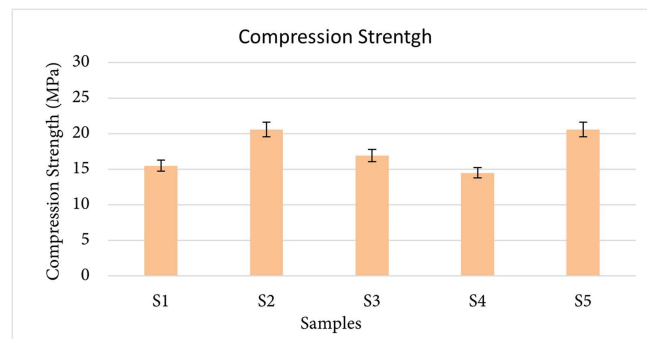


Figure 19. Compression strength.

3.7. Microscopy Analysis

Microscopic analysis was performed to investigate the distribution of chicken feather powder (CFP) and chicken feather fibers (CFF) in the PHA matrix, as well as to examine fracture morphologies after mechanical testing. The left-side images illustrate filler dispersion within the composite, while the right-side images show corresponding fracture surfaces. High-resolution microscopy enabled detailed observation of voids, cracks, filler alignment, agglomeration, and interfacial bonding, which directly influence mechanical properties such as strength, fracture toughness, and impact resistance.

3.7.1. PHA 90% + CFP 10%

Figure 20(a) shows the dispersion of 10% CFP in the PHA matrix, demonstrating a largely uniform particle distribution with only minor voids. **Figure 20(b)** illustrates the fracture surface, with arrows indicating stress concentration sites, uniform dispersion, and small porosity.

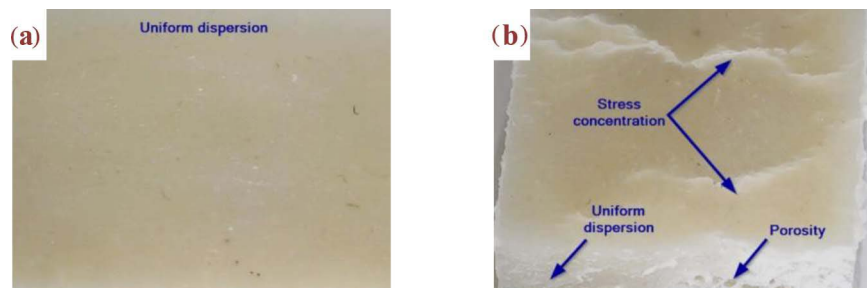


Figure 20. PHA-CFP (10%) composite morphology: (a) CFP dispersion in PHA, (b) Fracture morphology of the composite.

These characteristics suggest that cracks may propagate relatively smoothly, resulting in brittle fracture. Consequently, tensile strength can be maintained, whereas fracture toughness and impact resistance are likely lower compared to fiber-reinforced composites.

3.7.2. PHA 80% + CFP 20%

Figure 21(a) shows the dispersion of 20% CFP in the PHA matrix. Arrows and circles highlight the agglomeration of powder and smaller rachis particles, indicating that CFP clusters can disrupt matrix continuity and create weak zones. **Figure 21(b)** depicts the fracture surface, with arrows pointing to voids, crack initiation sites, and poorly dispersed regions, which can lead to increased stress concentration and rapid crack propagation, resulting in markedly brittle fractures. Consequently, the high CFP content significantly reduces tensile strength, increases brittleness, and lowers impact toughness due to these microstructural defects.

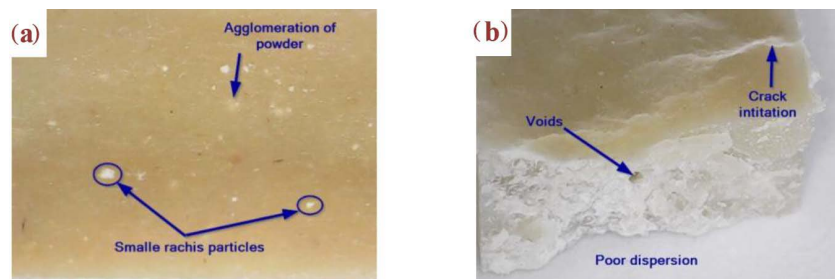


Figure 21. PHA-CFP (20%) composite morphology: (a) CFP dispersion in PHA, (b) Fracture morphology of the composite.

3.7.3. PHA 90% + CFF 10%

Figure 22(a) shows the dispersion of 10% CFF in the PHA matrix. Arrows highlight the presence of large rachis particles, while the overall uniform dispersion indicates that the elongated fibers are moderately well aligned and bonded to the polymer matrix. However, the larger rachis particles can act as stress concentrators, potentially initiating microcracks under load.

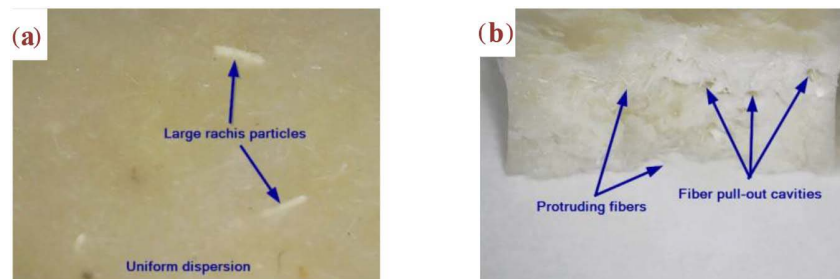


Figure 22. PHA-CFF (10%) composite morphology: (a) CFF dispersion in PHA, (b) fracture morphology of the composite.

Figure 22(b) shows the fracture morphology of the composite, highlighting

protruding fibers and fiber pull-out cavities. These features suggest that while the fibers contribute to stress transfer and reinforcement, the presence of fiber pull-out cavities may reduce energy absorption and fracture toughness. Overall, moderate fiber loading promotes alignment and bonding, but careful control of fiber size and dispersion is essential to minimize stress concentration and optimize mechanical performance.

3.7.4. PHA 80% + CFF 20%

Figure 23(a) shows the dispersion of CFF at 20% loading, with arrows highlighting large rachis particles and areas of poor dispersion. This indicates that fiber networks can become dense, agglomerated, and generate voids around clusters. **Figure 23(b)** depicts the fracture surface, with arrows indicating protruding fibers and fiber pull-out cavities. These features demonstrate that fibers can bridge cracks and be extracted, creating energy-absorbing sites. Although processing-induced thick and long fibers may create local stress concentrations, the extensive fiber pull-out and crack-bridging mechanisms significantly improve fracture toughness, tensile strength, and impact performance compared to CFP-filled composites.

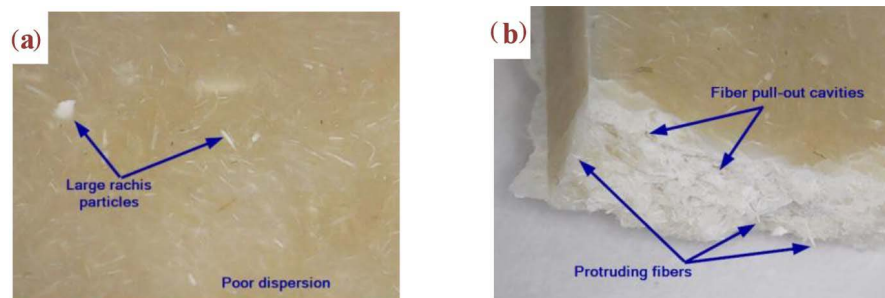


Figure 23. PHA-CFF (20%) composite morphology: (a) CFF dispersion in PHA, (b) Fracture morphology of the composite.

Overall, microscopy demonstrates the contrasting behavior of powder versus fiber reinforcement: CFP composites are prone to agglomeration and void formation, particularly at higher loadings, which could lead to brittle fractures and reduced mechanical properties, whereas CFF composites exhibit better alignment, stronger interfacial bonding, and energy-absorbing pull-out mechanisms that could enhance toughness and impact resistance.

4. Discussion

The mechanical performance data clearly demonstrate that both the morphology and concentration of feather fillers critically influence the behavior of PHA-based composites. Tensile testing showed that CFP provided moderate reinforcement, while higher loadings (20%) led to variability in strength, likely due to particle agglomeration and weak matrix-particle bonding. In contrast, 20% CFF exhibited the highest tensile strength, indicating that high-aspect-ratio fibers enhance stress

transfer and matrix interlocking. Alkali and silane treatments improved interfacial adhesion by introducing reactive groups and increasing surface roughness, which strengthened bonding between the feather fillers and the PHA matrix.

Trends in Young's modulus, Shore A and D hardness, compression strength, and density further highlight the influence of filler morphology and concentration. CFP at low loading slightly increased the modulus, but higher concentrations reduced stiffness, likely due to agglomeration disrupting matrix continuity. CFF composites showed a slightly lower modulus but improved Shore A hardness, indicating that fibers enhance surface load-bearing capacity. Compression testing revealed that 20% CFF increased compressive strength while reducing density by approximately 7%, consistent with the hollow fiber structure and demonstrating potential for lightweight, mechanically reliable composites. CFP composites, while improving compressive strength at 10%, may underperform at higher concentrations due to particle clustering.

Microscopy analysis provides mechanistic insights into these trends. CFP composites displayed particle clustering and voids, which might explain their reduced mechanical reliability, whereas CFF composites exhibited aligned fibers, strong interfacial bonding, and fiber pull-out, contributing to enhanced tensile strength and toughness. These observations confirm that fiber morphology, chemical treatment, and optimized filler loading are critical determinants of composite performance. Overall, CFF consistently outperformed CFP, demonstrating that the combination of appropriate filler morphology, concentration, and surface modification can effectively transform chicken feather waste into a functional reinforcement phase for sustainable, biodegradable PHA composites.

Although alkali and silane treatments improved interfacial adhesion and enhanced the mechanical performance of the composites, it should be noted that the silane coating may affect the biodegradability of the final material. The organosilane layer can create a partially hydrophobic barrier on the feather fibers, which may slow microbial degradation and reduce the overall decomposition rate of the PHA-based composites. This represents a potential limitation, highlighting a trade-off between mechanical durability and environmental degradability. Future studies should aim to optimize surface treatments to balance improved mechanical properties with the preservation of biodegradability.

5. Conclusion

In conclusion, this study demonstrates that chicken feather waste can effectively reinforce biodegradable PHAlife™ PB3430G composites when processed as fibers (CFF) or powders (CFP) with alkali and silane surface treatments. The 20% CFF composite (S5) exhibited the highest mechanical performance, achieving a tensile strength of 15.7 MPa (an 8% increase over neat PHA) and a Shore A hardness improvement of 6.5% - 8.3%, while reducing density by approximately 7%. Microscopic analysis revealed well-aligned fibers, pull-out mechanisms, and minimal void formation, which collectively explain the enhanced stress transfer and

mechanical reinforcement observed. Powdered feathers provided moderate reinforcement at low loadings but caused agglomeration and voids at higher contents, limiting their effectiveness. These findings confirm that feather morphology, optimized concentration, and chemical surface treatment synergistically improve the mechanical and physical properties of PHA composites. Overall, this work highlights a sustainable and biodegradable approach to valorizing poultry feather waste, offering lightweight, mechanically robust materials suitable for consumer goods and agricultural applications. These results are specific to the PHALife™ PB3430G matrix, feather fillers, and compression molding process used, and may differ with other materials or processing methods.

6. Future Scope

Future studies should focus on evaluating the biodegradation behavior of these composites. Further optimization of surface modification techniques, such as enzymatic or bio-based treatments could enhance fiber matrix compatibility and mechanical properties. Conducting life cycle assessments and cost-benefit analyses will help determine the commercial scalability and environmental impact. Additionally, exploring real-world applications in packaging, agriculture, and lightweight consumer products will support the transition of these materials from laboratory research to industrial deployment.

Acknowledgements

The author acknowledges Hochschule Kaiserslautern, Department of Applied Logistics and Polymer Sciences, Pirmasens, Germany, for providing funding and research facilities. Sincere appreciation is extended to Prof. Jens Schuster for his guidance and valuable input, and to Assistant Prof. Chandrasekhar Kode for his support throughout the study. Their contributions have been instrumental in advancing this work on sustainable polymer composites.

Conflicts of Interest

The authors declare no conflicts of interest regarding the publication of this paper.

References

- [1] Nguyenhuynh, T., Yoon, L.W., Chow, Y.H. and Chua, A.S.M. (2021) An Insight into Enrichment Strategies for Mixed Culture in Polyhydroxyalkanoate Production: Feedstocks, Operating Conditions and Inherent Challenges. *Chemical Engineering Journal*, **420**, Article ID: 130488. <https://doi.org/10.1016/j.cej.2021.130488>
- [2] Chen, G. (2009) A Microbial Polyhydroxyalkanoates (PHA) Based Bio- and Materials Industry. *Chemical Society Reviews*, **38**, 2434-2446. <https://doi.org/10.1039/b812677c>
- [3] Dutta, H., Bora, D., Chetia, P., Bharadwaj, C., Purbey, R., Bohra, R.C., *et al.* (2024) Biopolymer Composites with Waste Chicken Feather Fillers: A Review. *Renewable and Sustainable Energy Reviews*, **197**, Article ID: 114394. <https://doi.org/10.1016/j.rser.2024.114394>

- [4] Aranberri, I., Montes, S., Azcune, I., Rekondo, A. and Grande, H. (2017) Fully Biodegradable Biocomposites with High Chicken Feather Content. *Polymers*, **9**, Article No. 593. <https://doi.org/10.3390/polym9110593>
- [5] Reddy, N. and Yang, Y. (2007) Structure and Properties of Chicken Feather Barbs as Natural Protein Fibers. *Journal of Polymers and the Environment*, **15**, 81-87. <https://doi.org/10.1007/s10924-007-0054-7>
- [6] Tesfaye, T., Sithole, B., Ramjugernath, D. and Chunilall, V. (2017) Valorisation of Chicken Feathers: Characterisation of Physical Properties and Morphological Structure. *Journal of Cleaner Production*, **149**, 349-365. <https://doi.org/10.1016/j.jclepro.2017.02.112>
- [7] Barone, J.R. and Schmidt, W.F. (2005) Polyethylene Reinforced with Keratin Fibers Obtained from Chicken Feathers. *Composites Science and Technology*, **65**, 173-181. <https://doi.org/10.1016/j.compscitech.2004.06.011>
- [8] Ali, A., Shaker, K., Nawab, Y., et al. (2018) Hydrophobic Treatment of Natural Fibers and Their Composites—A Review. *Journal of Industrial Textiles*, **48**, 725-763.
- [9] Khan, A., Parikh, H. and Qureshi, M.R.N. (2022) A Review on Chicken Feather Fiber (CFF) and Its Application in Composites. *Journal of Natural Fibers*, **19**, 12565-12585.
- [10] Adekunle, K.F. (2015) Surface Treatments of Natural Fibres—A Review: Part 1. *Open Journal of Polymer Chemistry*, **5**, 41-46.
- [11] Ali, M.F., Hossain, M.S., Moin, T.S., Ahmed, S. and Chowdhury, A.M.S. (2021) Physico-Mechanical Properties of Treated Chicken Feather-Reinforced Unsaturated Polyester Resin Based Composites. *Nano Hybrids and Composites*, **32**, 73-84. <https://doi.org/10.4028/www.scientific.net/nhc.32.73>
- [12] Amieva, E.J., Velasco-Santos, C., Martínez-Hernández, A., Rivera-Armenta, J., Mendoza-Martínez, A. and Castaño, V. (2014) Composites from Chicken Feathers Quill and Recycled Polypropylene. *Journal of Composite Materials*, **49**, 275-283. <https://doi.org/10.1177/0021998313518359>
- [13] Bharathi, S.V. and Raj, I.V. (2021) Studies on the Physical Properties of Chicken Feathers. *International Journal of Current Microbiology and Applied Sciences*, **10**, 309-315.
- [14] Xie, Y., Hill, C.A.S., Xiao, Z., Militz, H. and Mai, C. (2010) Silane Coupling Agents Used for Natural Fiber/Polymer Composites: A Review. *Composites Part A: Applied Science and Manufacturing*, **41**, 806-819. <https://doi.org/10.1016/j.compositesa.2010.03.005>
- [15] Oladele, I.O., Okoro, A.M., Omotoyinbo, J.A. and Khoathane, M.C. (2018) Evaluation of the Mechanical Properties of Chemically Modified Chicken Feather Fibres Reinforced High Density Polyethylene Composites. *Journal of Taibah University for Science*, **12**, 56-63. <https://doi.org/10.1080/16583655.2018.1451103>
- [16] Paşayev, N., Tekoğlu, O., Kocatepe, S., Erol, M. and Maraş, N. (2021) The Machine Method for Processing Chicken Feathers by Splitting Them into Fibers and Rachis. *Tekstil ve Mühendis*, **28**, 248-260. <https://doi.org/10.7216/1300759920212812401>
- [17] Cheng, S., Lau, K., Liu, T., Zhao, Y., Lam, P. and Yin, Y. (2009) Mechanical and Thermal Properties of Chicken Feather Fiber/PLA Green Composites. *Composites Part B: Engineering*, **40**, 650-654. <https://doi.org/10.1016/j.compositesb.2009.04.011>
- [18] Touatou, S. and Belhaneche-Bensemra, N. (2021) Valorisation of Chicken Feather Fibres in Developing Poly(vinyl chloride) Biocomposites.
- [19] Tesfaye, T., Sithole, B., Ramjugernath, D. and Chunilall, V. (2017) Valorisation of Chicken Feathers: Characterisation of Chemical Properties. *Waste Management*, **68**,

626-635. <https://doi.org/10.1016/j.wasman.2017.06.050>

- [20] Helian Polymers (2025) PB3430G (P34HB) Technical Datasheet.
<https://shop.helianpolymers.com/products/pb3430g-p34hb-15-4-hb-pellets>